

## A Heat Flux Sensor to Monitor Composite Manufacturing Processes

Maxime Villière, Xavier Tardif, Sebastien Guérout, Vincent Sobotka, Nicolas Boyard, Didier Delaunay, Joël Bréard

► **To cite this version:**

Maxime Villière, Xavier Tardif, Sebastien Guérout, Vincent Sobotka, Nicolas Boyard, et al.. A Heat Flux Sensor to Monitor Composite Manufacturing Processes. Le Cam, Vincent and Mevel, Laurent and Schoefs, Franck. EWSHM - 7th European Workshop on Structural Health Monitoring, Jul 2014, Nantes, France. 2014. <hal-01020393>

**HAL Id: hal-01020393**

**<https://hal.inria.fr/hal-01020393>**

Submitted on 8 Jul 2014

**HAL** is a multi-disciplinary open access archive for the deposit and dissemination of scientific research documents, whether they are published or not. The documents may come from teaching and research institutions in France or abroad, or from public or private research centers.

L'archive ouverte pluridisciplinaire **HAL**, est destinée au dépôt et à la diffusion de documents scientifiques de niveau recherche, publiés ou non, émanant des établissements d'enseignement et de recherche français ou étrangers, des laboratoires publics ou privés.

## A heat flux sensor to monitor composite manufacturing processes

Maxime Villière<sup>1</sup>, Xavier Tardif<sup>2</sup>, Sébastien Guérault<sup>2</sup>, Vincent Sobotka<sup>1</sup>,  
Nicolas Boyard<sup>1</sup>, Didier Delaunay<sup>1</sup>, Joël Bréard<sup>3</sup>

<sup>1</sup>Laboratoire de thermocinétique, UMR CNRS 6607, Ecole Polytechnique de l'université de Nantes, La Chantrerie, Rue Christan Pauc, 44306 Nantes Cedex 03, France.

<sup>2</sup>IRT Jules Verne, Chemin du Chaffault, 44340 Bouguenais

<sup>3</sup>Université du Havre, Laboratoire d'Ondes et Milieux Complexes, CNRS UMR 6294, 53 rue de Prony, BP 540, 76600 Le Havre, France

Corresponding author: sebastien.guerault@irt-jules-verne.fr

### ABSTRACT

Composite materials are heterogeneous materials which consist of a matrix reinforced by fibers. One of the most promising manufacturing processes are Liquid Composite Moulding (LCM) in which a stationary fibrous preform is impregnated by a liquid. It is essential to monitor two key-steps in order to ensure high quality composite parts: the mould-filling stage, during which the liquid resin flows through the fibrous preform and the solidification. Two examples related to these issues are detailed here, the common point being the use of the same sensor to identify the different properties. In a first part, an experimental device has been designed to quantify the saturation profile of a preform. This set-up consists of a mould with heat flux sensors and an injection device reproducing the actual forming process. The saturation curve can be obtained by exploiting the wall heat fluxes. In a second part, this study emphasizes the use of the same heat flux sensors to monitor the consolidation phase. Indeed heat transfer and temperature during the forming process are strongly coupled with the phase change through the variation of thermal properties. These methods clearly open up new perspectives regarding the online control of composite manufacturing processes at an industrial scale.

Keywords: *Heat Flux, Composite manufacturing, Sensors, Monitoring.*

### 1. INTRODUCTION

Composite materials are heterogeneous materials which generally consist of a matrix reinforced by fibers. These materials are distinguished by their outstanding “strength-to-weight” ratio. As a result, they represent ideal substitutes to metallic parts. Resin Transfer Moulding (RTM) is part of the Liquid Composite Moulding (LCM) family. RTM process refers to the placement of dry fabrics in a rigid mould followed by the impregnation of the resulting preform by a thermosetting or thermoplastic resin. RTM process uses the low viscosity resins to insure a proper impregnation of large parts with a high fibre volume fraction. This is an increasingly used process for producing complex composite structural parts in many domains such as automotive or aeronautics. During this process, it is essential to monitor two key-steps in order to ensure high quality composite parts.

The first key step is the mould-filling stage, during which the liquid resin flows through the fibrous preform. Due to the dual scale of porosity in a fiber preform there is formation of “voids” which are gas bubble entrapped in the preform during the impregnation [1], [2]. Authors [3] have shown their detrimental influence on the mechanical properties of the composite. The monitoring of their creation and transport thus represents an undeniable advantage. The second key step is the

consolidation of the preform. The chemical reactions being exothermal, the variation in thermal response can be greatly significant. Indeed, the heat transfers in the composite parts are strongly coupled with the phase change. Moreover, the problem becomes nonlinear due to the variation of the thermal properties [4]. The monitoring of the heat transfer is mandatory to follow the curing phase of the composite part.

The physical and chemical phenomena which occur throughout these two steps are strongly coupled to heat transfer. Therefore, it is necessary to monitor heat fluxes and temperatures in order to control the process. Thus the aim of this study is to present the use of heat flux sensors to monitor all the keys steps of the processes. The first part will describe the heat flux sensors used during the experiments. The second and third parts will detail the use of the sensors to monitor respectively the mould filling stage and the consolidation stage on experimental devices. The last part will conclude on the use of the sensor and the new perspectives regarding the online control of composite manufacturing processes at an industrial scale.

## 2. HEAT FLUX SENSORS

There is a few types of sensors used to monitor composite manufacturing process, but the common one are: temperature sensors, pressure sensors, dielectric sensors and heat flux sensors. This part relates the basic theoretical aspects of the heat flux sensors used to monitor composite processes [5]. The sensor is made of three thermocouples located at different position. The wires of thermocouple follow the isothermal lines which are parallel to the surface on which heat transfers are quantified. The hot junctions are aligned according to the normal to this surface (Figure 1). The post-processing of the temperature recordings carried out by the thermocouples is done by a one-dimensional inverse heat conduction problem with Beck sequential algorithm in a material with known thermal conductivity [6]. To solve the problem, the temperature given by the third thermocouple is used as a boundary condition and the temperature given by the first and second thermocouple constitutes the additional information necessary to the resolution. A schema of the sensor is exposed in Figure1. According to the functioning of the sensor, the wall temperature and the heat flux density can be measured.

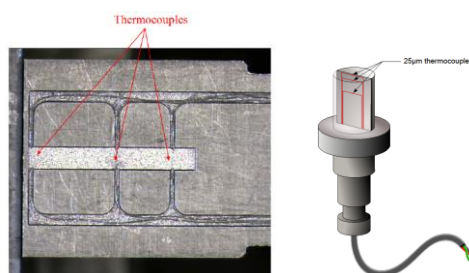


Figure 1: Heat flux sensor [4]

One of the main concerns about the heat flux sensors are their thermal intrusivity. To assure a minor impact on the heat flux measured, the body of the sensor is made of the same materials to those of the mould or experimental device.

## 3. MOULD-FILLING STAGE MONITORING

### 3.1. Experimental devices and experimental protocol

An experimental bench was used to model 1D injection in a fiber preform (see Figure 2). It includes an injection system and a mould made of three parts. The upper mould is made of glass allowing a direct visual control during the impregnation. The lower part of the mould is a steel plate with an adjustable vertical position to quantify the fiber volume fraction. An aluminium heat exchanger is in

contact with the lower face of the steel plate. The heat released during the experiment is absorbed by the water circulation of a laboratory thermostat maintaining a constant temperature. Finally an injection device containing the model liquid allows an accurate control of the fluid flow rate. Regarding the monitoring devices, three heat flux sensors are integrated in the lower plate of the mould and three tangential gradient heat flux sensors are located on the top of the glass part to monitor the heat losses through the upper mould. The first ones record the thermal response of the system through the transverse wall heat flux.

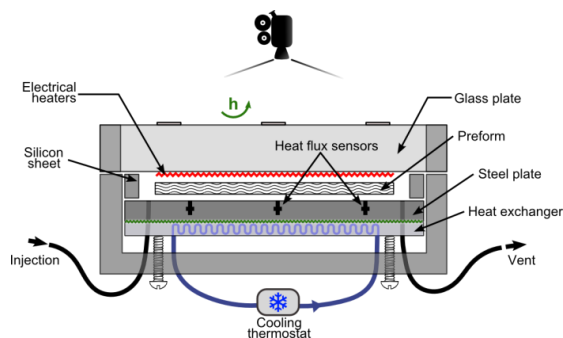


Figure 2: Schematic view of the mould and its sensors

All the experiments are injections of a model liquid through the length of a unidirectional glass fabric. The injections are performed at constant flow rate. The model liquid has been selected due to its properties close to those of a classical resin used during RTM process. Some key-temperatures are monitored during the experiment such as the evolution of the temperature of the fluid before injection,  $T_{inlet}$  to ensure an isothermal condition. During the experiment, the heaters are turned on as soon as the model liquid reached the fiber preform and the power supplying of the heater is kept constant. In order to calibrate the system and estimate the thermal boundaries conditions, preliminary experiments were performed. These experiments were conducted with fluid only or dry preform only and the results are exposed in Table 1.

Table 1 Thermophysical properties and estimated boundary conditions of the experimental bench. Temperature dependence of the conductivities of air and liquid has been taken into account.

	$\rho$ ( $kg.m^{-3}$ )	$C_p$ ( $J.kg^{-1}.K^{-1}$ )	$\lambda$ ( $W.m^{-1}.K^{-1}$ )	$h$ ( $W.m^{-2}.K^{-1}$ )
Glass plate	2550	803	1.1	7
Glass fiber	2550	803	1.0	--
Air	1.2	1006	F(T)*	--
Model liquid	1226	2434	F(T)**	--
Metal	7850	460	35	--

$$\lambda_{air} = 1.52.10^{-11}T^3 - 4.86.10^{-8}T^2 + 1.02.10^{-4}T - 3.93.10^{-4}$$

$$\lambda_{liquid} = 8.08.10^{-6}T^2 - 1.33.10^{-4}T + 0.34 \text{ (Measured by Hot Disk method)}$$

### 3.2. Experimental results

The experiments were performed at a constant flow rate of  $2.1 \text{ mL/min}$  and  $4.2 \text{ mL/min}$ . The experimental wall heat fluxes for the first experiment have been plotted in Figure 3. As shown in the figure, the heaters are turned on at  $t=0$ , when the liquid reach the very beginning of the preform. The constant heat flux density dissipated is close to  $1600 \text{ W/m}^2$ . As long as the liquid front stays behind the first sensor the problem is reduced to a simple 1D-conduction problem that is why the three heat flux sensors responses are roughly the same. When the liquid front reaches the sensors each data recording shows a sudden variation of heat flux density which can be linked with the variation of saturation in the fibrous preform.

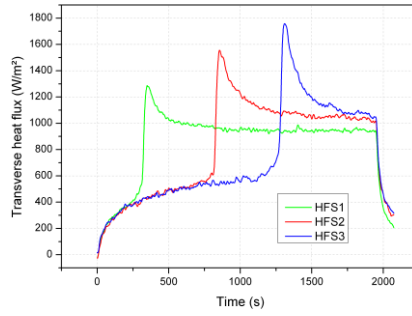


Figure 3: Experimental wall heat fluxes for each sensor during the injection.

### 3.3. Saturation monitoring

The variation of saturation in the fibrous preform, from an unsaturated state ( $S=0$ ) to a saturated state ( $S_T \sim 1$ ) changes significantly the thermal properties of the porous medium. As a consequence, the experimental results (figure 3) are strongly impacted by the arrival of the liquid. In order to obtain the evolution of the saturation during the experiments, three key-steps are needed. The first one is the description of heat transfer in the porous medium which can be modeled in a simplified manner by the following equation:

$$\left( \rho C_p(S_T(x, t)) \right) \frac{\partial T}{\partial t} + \left( \rho C_p(S_T(x, t)) \right) \bar{u} \bar{\nabla T} = \bar{\nabla} \cdot \left( \lambda(S_T(x, t)) \bar{\nabla T} \right) \quad (1)$$

where  $\bar{u}$  is the average interstitial velocity of the fluid,  $S_T$  the global saturation of the porous medium,  $\rho$  the density,  $\lambda_x$  the in-plane thermal conductivity and  $C_p$  the specific heat capacity. The in-plane thermal conductivity  $\lambda_x$  as well as the thermal inertia ( $\rho C_p$ ) are modeled by a straightforward rule of mixtures (Equation 2 and 3). These two equations imply a linear variation between the unsaturated state ( $S_T=0$ ) and the fully-saturated one ( $S_T=1$ ). The values at the limits are issued from experimental measurements [7].

$$\lambda_x(S_T) = (\lambda_x)_{S_T=0} + S_T \left[ (\lambda_x)_{S_T=1} - (\lambda_x)_{S_T=0} \right] \quad (2)$$

$$(\rho C_p)(S_T) = (\rho C_p)_{S_T=0} + S_T \left[ (\rho C_p)_{S_T=1} - (\rho C_p)_{S_T=0} \right] \quad (3)$$

The second key-step is the determination of the transverse thermal conductivity as a function of the saturation. A sensitivity analysis showed that this parameter strongly impacts heat transfers. As it is not possible to measure experimentally this property for a known porosity, a modelling was required. Then, a representative elementary volume which described the morphology of the preform and the transverse thermal conductivity was defined. The model was developed using a homogenization methodology in order to describe the thermal behavior of the porous medium during the injection. As said before a fibrous preform is a dual scale porous media leading to the formation of micro-voids, which appear inside tows, and macro-voids which appear between each tow. Hereinafter, two different saturations are considered: the micro-saturation  $S_\mu$ , defined as the intra-tows saturation and the macro-saturation  $S_M$ , defined as the saturation between tows. A linear relationship is used to link multi-scale saturation with the total saturation, where  $\phi_f^c$  represents the fiber volume fraction, and  $\phi_t^c$  the tow volume fraction in the composite.

$$S_T = \left( \frac{\phi_t^c - \phi}{1 - \phi_f^c} \right) S_\mu + \left( \frac{1 - \phi_t^c}{1 - \phi_f^c} \right) S_M \quad (4)$$

Assuming that the preform possesses a dual scale pore morphology, two representative elementary volumes have been built (see Figure 4.a). The saturation at each scale has been modeled by growing air bubbles within tows, or in the inter-tow area. A homogenization method has been performed sequentially at the two scales, with periodic boundary conditions over the edges of the unit cell. The effective thermal transverse conductivity has been computed for all possible ratios of micro-saturation and macro-saturation. Thus the convection-diffusion equation can be solved and gives us the evolution of the transverse thermal conductivity in the mould.

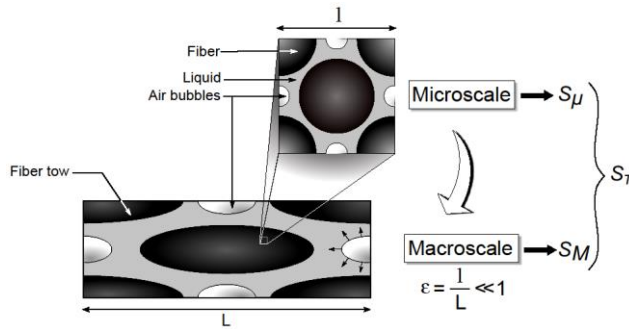


Figure 4: Representative elementary volume at microscale and macroscale and effective thermal conductivity as a function of the saturation.

The last part is the definition of the saturation profile. Many researchers showed, either by experimental measurements or modeling [8][9] that the saturation of a fibrous preform by a liquid was described by a characteristic curve such as the one depicted in figure 5. This latter is modeled using several constant geometric parameters: the length of the unsaturated front ( $l$ ), the value of saturation at the slope change ( $y_i$ ), and the maximal saturation at the beginning of the preform ( $S_{max}$ ).

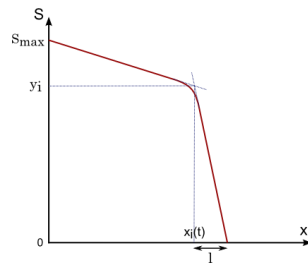


Figure 5: Modeling of the saturation curve as a function of geometric parameters  $l$ ,  $y_i$ , and  $S_{max}$ .

The saturation curve parameters are then determined by minimizing the cost function defined as the square difference between the measured and computed wall heat flux (Equation 5) where  $n$  is the number of time step,  $k$  the sensor number,  $\tilde{\varphi}$  the experimental transverse heat flux, and  $\varphi$  the computed transverse heat flux.

$$J(S_{max}, y_i, l) = \sum_n \sum_{k=1}^3 (\tilde{\varphi}_k^n - \varphi_k^n)^2 \tag{5}$$

The following figure represents the computed saturation for two different flow rates.

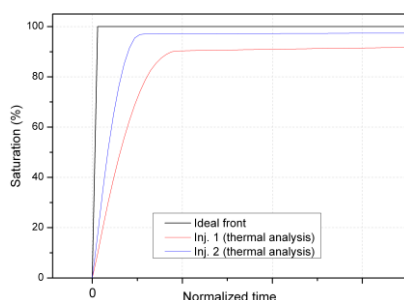


Figure 6: Theoretical and experimental saturation for two different injection conditions.

The obtained saturation curves can be compared with measure obtained by a well-trieed method *i.e.* the conductometric sensor [2][9]. The results are consistent with each other. The experimental results confirm that there is a difference between the ideal saturation and the saturation obtained by the thermal analysis and that the fiber preform remains partially saturated with a saturation profile depending on the injection parameters. The information obtained are indeed useful to monitor the injection process. In one case the maximum saturation remains close to 0.91 leading to a “massive” void content whereas the second injection can be considered fully saturated with a saturation of 0.98 at the end of the experiment.

## 4. CONSOLIDATION STAGE MONITORING

### 4.1. Experimental devices and experimental protocol

The PVT $\alpha$  mould used in this work is a home-made apparatus. It consists of a piston which can move in a cylindrical stainless steel cavity (Figure 7) in which polymer sample is placed beforehand. The sample is about 6mm thick and 40mm in diameter. The mould is placed between two platens of an electric press that adjusts, in real time, the position of the piston to keep constant the applied pressure (from 0.5 MPa to 10 MPa) on the sample.

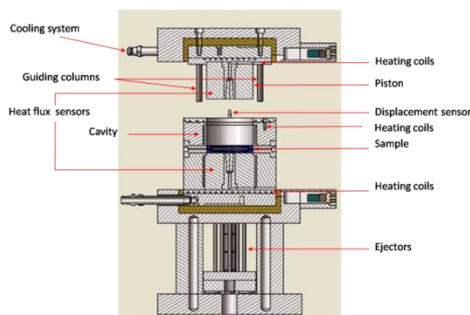


Figure 7: PVT apparatus

The mould is designed so that heat transfer is 1D through the sample thickness unlike classical PVT. The heating is ensured by three electric heaters located at the top and bottom to heat the piston and cavity respectively. The cooling system consists of compressed air circulating in the top and in the bottom of the mould. This device is instrumented with two heat flux sensors, one in the piston and the other in the moulding cavity. Volume variations are recorded by LVDT-type displacement sensor. A complete description of this device is given in [4].

### 4.2. Thermoset resin curing

The relevance of the heat flux sensor to follow chemical reactions has been illustrated by Dupuy *et al* [10]. In this paper, authors aimed to follow the crosslinking kinetics of unsaturated polyester

resin containing a large excess of styrene. The PvT $\alpha$  apparatus coupled with a Matrasur Starmed 5000 RTM machine has been used to simulate the RTM process. The predefined ratio of catalyst is added in the injection head of the machine just before the formulation enters the static mixer. A heating device ensures the thermoregulation of the whole circuit, i.e. from the tank to the head injection, so that the resin can be injected exactly at the mould temperature.

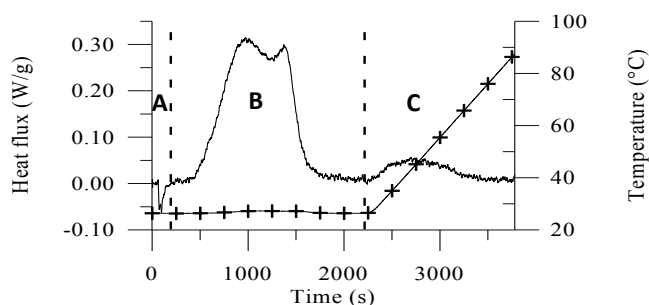


Figure 8: Recorded heat flux and heat-up ramp.

The figure shows the temperature and the heat flux recorded by the heat flux sensor from the injection of the resin in the mould to the end of the heating. The cycle is composed of three parts: the first one corresponds to the injection of the resin (A), the second one to the isothermal curing (B) and the third one to the post-curing (C). In the A area, the variation of the flux is due to the injection of resin, which is not totally isothermal. The negative value proves that the resin and probably the air contained in the duct at the beginning of injection is colder than the moulding cavity. In the B zone, after the injection heat flux comes back to zero, proving a thermal equilibrium between the resin and the mould. Then, the exothermic reaction takes place. Two peaks are present on the heat flux curve because of a chemical reaction in the resin. The heat flux value is back to zero after the end of the crosslinking. Finally (Zone C) a heating is imposed to the sample so as to post-cure it. The small peak that appears proves clearly that the chemical reaction was not complete in phase B. Integration of the peak leads directly to the degree of cure of the resin. This type of sensor can be then an efficient mean to quantify in real time the crosslinking, provided that the released energy can be detected.

#### 4.3. Semi-crystalline polymer crystallization

In this part, the cooling of an isotactic Polypropylene in the PvT $\alpha$  mould is recorded [11]. The temperature of the sample is measured with a K type thermocouple inserted exactly in the middle of the polymer part. The heat flux and the temperature of the mould are also recorded. All these data are presented in the Figure 9.

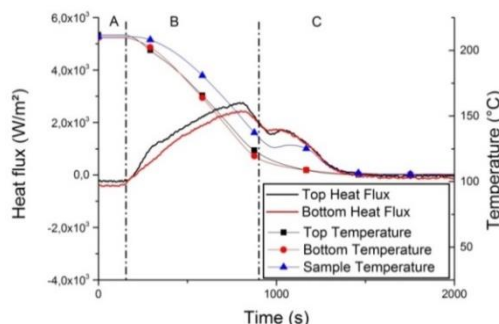


Figure 9: Cooling from 220 °C to 100°C of an iPP

The figure 9 presents the cooling of the polymer from 220°C to 100°C at 10K/min. The thermogram shows three different areas. In the first part, the polymer is at 220°C and the heat flux is constant



and close to zero. Then, the polymer is cooled down and the heat flux increases. In this zone, the boundaries of the polymer are 20°C colder than the middle. In the C area, the temperature of the sample increases and the heat flux presents a small increase because the polymer crystallizes. However, the temperature of the mould part is not sensitive to the crystallization. The two previous examples clearly shows the heat flux is a relevant information to detect the phase change during the material forming whereas we also observed the temperature of the mould is not sensitive.

## CONCLUSION

Due to the complexity of the injection step during liquid composite molding processes, composite parts are prone to defects leading to a decrease of their mechanical properties. Thus, *in situ* monitoring is one of the key-objectives to control these manufacturing processes. In order to respond to this problematic many sensors may be used, like pressure, dielectric or temperature sensors, but the information obtained is not sufficient or tricky to exploit. That is why two innovative methods using heat flux sensors were proposed. The first one relies on the measurement of wall heat flux to determine the saturation of a fibrous preform during injection. The dynamic saturation curves of a fibrous preform at different injection conditions have been successfully measured despite the use of some assumptions. The second one is widely used in experimental moulds and characterization devices, and shows clearly that heat fluxes are relevant to monitor chemical reactions. However, these two methods are performed in laboratory conditions and their use in an industrial context remains a technological bottle-neck. Nevertheless this paper clearly opens up new perspectives regarding the online control of composite manufacturing processes at an industrial scale.

## REFERENCE

- [1] N. Patel. Micro-scale flow behavior, fiber wetting and void formation in liquid composite moulding. Ohio State University, 1994.
- [2] S. Guérout, L. Bizet, J. Bréard. Experimental determination of void formation and transport in the RTM process. in *FPCM II*, 111–118., July 2012.
- [3] J. Varna, R. Joffe, A. Berglund, T. S. Lundström. Effects of voids on failure mechanisms in RTM laminates. *Composites Science and technology*, 53:241-249, 1995
- [4] X. Aduriz, C. Lupi, N. Boyard, J. Bailleul, D. Leduc, V. Sobotka, N. Lefevre, X. Chapeleau, C. Boisrobert, D. Delaunay. Quantitative control of RTM6 epoxy resin polymerisation by optical index determination. *Composites Science and Technology*, 67:3196-3201, December 2007.
- [5] B. Bourouga, V. Goizet, J. P. Bardon. Les aspects théoriques régissant l'instrumentation d'un capteur thermique pariétal à faible inertie. *International Journal of Thermal Sciences*, 39:96-109, 1999.
- [6] J. V. Beck, B. Blackwell, C. R. ST. Jr Clair. Inverse heat conduction III-Posed Problems. *Wiley-inte edition*, 1985.
- [7] M. Villière, D. Lecointe, V. Sobotka, N. Boyard, D. Delaunay. Experimental determination and modeling of thermal conductivity tensor of carbon/epoxy composite. *Composite Part A: Applied Science and Manufacturing*, 46:60-68, Nov. 2012.
- [8] M. Nordlund, V. Michaud. Dynamic saturation curve measurement for resin flow in glass fibre reinforcement. *Composites Part A: Applied Science and Manufacturing*, 43:333–343, Mar. 2012.
- [9] S. Guerout, A. Lebel-Lavacry, C. H. Park, L. Bizet, S. Abdelghani, J. Bréard. Analytical modeling and in situ measurement of void formation in liquid composite moulding processes. *Advanced Composite Materials*. 23, 2014.
- [10] J. Dupuy, J. Adami, A. Maazouz, V. Sobotka, D. Delaunay. Kinetic modeling of unsaturated polyester resin using two complementary techniques: Near Infra Red spectroscopy and heat flux sensors. *Polymer Engineering & Science*, 45:846-856, June 2005.
- [11] X. Tardif, A. Agazzi, V. Sobotka, N. boyard, Y. jarny, D. Delaunay. A multifunctional device to determine specific volume, thermal conductivity and crystallization kinetics of semi-crystalline polymers. *Polymer testing*. 6:819-827. Sep. 2012.